ELSEVIER

PII: S0032-3861(97)00361-3

Polymer Vol. 39 No. 4, pp. 821–834, 1998

0032-3861/97/$17.00+0.00

Fracture behaviour of polycarbonate blends with a core–shell impact modifier

Y. Kayano†, H. Keskkula and D. R. Paul*
Department of Chemical Engineering and Center for Polymer Research, University of Texas at Austin, Austin, TX 78712, USA
(Received 30 August 1995; revised 6 January 1996)

A detailed characterisation of the high speed fracture behaviour of polycarbonate/core–shell impact modifier blends using thick (6.25 mm) injection moulded bars with sharp notches via the Vu-Khanh methodology and data analysis is described. This expands on a previous report that examined the effect of polycarbonate molecular weight and melt blending conditions on the customary stress–strain and impact properties of such blends. Load–deflection curves and impact strength as a function of temperature are also reported. Morphological features near crack tips formed at high speed were examined by microscopy to gain insight about the sequence of events that occur during crack propagation. The use of thick specimens with sharp notches gives a better discrimination of how the concentration and degree of dispersion of impact modifier influence the toughness of these polycarbonate blends than does Izod testing using thin specimens with standard notches. High molecular weight of the matrix and good dispersion of the impact modifier in the matrix lead to both higher fracture energy at initiation and tearing modulus. Model calculations are presented to explain the different fracture responses under plane strain versus plane stress conditions caused by addition of impact modifier to polycarbonate. © 1997 Elsevier Science Ltd.

(Keywords: blends; polycarbonate; core–shell impact modifier)

INTRODUCTION

Addition of small amounts of core–shell impact modifier particles to bisphenol A polycarbonate (PC) leads to reduced notch sensitivity, toughness of thick sections and good low temperature toughness with only small sacrifices in tensile behaviour[1–3]. Several reports[4–13] describe the changes in these and other technologically important characteristics that result from blending core–shell impact modifiers with PC. An earlier paper described the effects of PC molecular weight, modifier concentration and blend preparation conditions on the degree of modifier dispersion, room temperature Izod impact strength, and the ductile–brittle transition temperature[14]. However, the standard notched Izod test is not an adequate method for fully characterising the toughening effects caused by the addition of a core–shell impact modifier to PC since the thin sections (3.13 mm) and the standard notch employed do not represent sufficiently severe fracture conditions to see the true benefits and to discriminate among possible blend morphologies. Furthermore, the Izod test only gives the total fracture energy for one ligament size. The purpose here is to report a more complete analysis of the fracture behaviour of these blends using a variety of techniques.

There is a rapidly growing body of literature on the use of fracture mechanics techniques to better characterise the toughness and to understand the deformation mechanisms that occur in toughened engineering thermoplastics[15–31]. The classical critical stress intensity factor (K_{IC}) from linear elastic fracture analysis requires very thick specimens to satisfy the small scale yield criterion[32,47] in materials with low yield strength and high toughness like polycarbonate and its blends. Such thick specimens cannot be formed easily by injection moulding which is a preferred method for fabricating plastic parts. It is now being recognised that techniques based on linear elastic fracture mechanics (LEFM) are not appropriate for such pseudo-ductile materials. For these reasons, the J-contour integral method has recently been regarded as more appropriate for such polymeric materials and has the benefit of not requiring exceedingly thick specimens[33,47]. However, the thickness required is still often beyond what can be conveniently injection moulded. Rigorous measurement of J_{IC} involves use of rather specialised equipment and techniques.

Vu-Khanh[24] recently proposed an approach for characterising fracture that offers a useful compromise between rigorous fracture mechanics methodology and the simplicity of Izod or Charpy measurements. In this method the energy, U, required to fracture a specimen with a ligament area, A, is measured by a standard or instrumented impact tester. It has the advantage of high test speeds found in impact conditions as opposed to essentially static loading conditions usually employed in J_{IC} measurements. The analysis of this type of data by the method proposed by Vu-Khanh yields a fracture energy at initiation, G_i, and a measure of the additional energy associated with propagating the fracture, or tearing modulus, T_a. Vu-Khanh proposed a model for this method of fracture characterisation for ductile polymers and claimed that the fracture energy at initiation, G_i, is equivalent to the critical J-integral for fracture, J_{IC}. Mai[34] pointed out that the Vu-Khanh approach is equivalent to the essential work analysis proposed by

* To whom correspondence should be addressed
† Permanent address: Mitsubishi Gas Chemical Co., 6-2 Higasi-Yahata, 5-Chome, Hiratsuka-shi 254, Japan

Table 1 Materials used in this study

Designation used here	Commercial designation	Form	Polycarbonate[a]	Brabender torque after 10 min (N·m) 260°C	290°C	Source
M-PC	Iupilon S3000	Pellet	$\bar{M}_n = 8500$			Mitsubishi Engineering-Plastics Corp.
	Iupilon S3000F	Flake	$\bar{M}_w = 23\,700$	9.7	4.7	
H-PC	Iupilon E2000	Pellet	$\bar{M}_n = 10\,800$			Mitsubishi Engineering-Plastics Corp.
	Iupilon E2000F	Flake	$\bar{M}_w = 32\,000$	19.3	10.6	
Core–shell impact modifier	HIA-28	Powder	–	14.5	16.5	Kureha Chemical Industry Co., Ltd.

[a]Determined by gel permeation chromatography using polystyrene standards

Mai, Williams, and others[22,35–37] and have questioned equating G_i to J_{IC}. Regardless of the interpretation used, this approach provides considerable useful information about the fracture process that goes well beyond the Izod or Charpy tests, both of which may be regarded as single point methods (one value of A) in this context.

The purpose of this paper is to expand on the previous report[14] that examined the effect of polycarbonate molecular weight and melt blending conditions on the customary stress–strain and impact properties of PC blends with core–shell impact modifiers. A detailed characterisation of high speed fracture behaviour of these blends using thick (6.25 mm) injection moulded bars with sharp notches is presented using the Vu-Khanh methodology and data analysis. The Vu-Khanh parameters are related to the degree of dispersion of the core–shell particles in polycarbonate. Transmission electron microscopy was also used to observe morphological features near crack tips that were arrested during high speed testing in order to understand the sequence of events that occur during crack propagation. It is shown that the degree of dispersion of the core–shell impact modifier particles, their concentration, and PC matrix molecular weight all have profound effects on the measured impact properties.

EXPERIMENTAL

Materials and process conditions

Two commercial molecular weight grades of polycarbonate from Mitsubishi Engineering-Plastics Corp. and a core–shell impact modifier from Kureha Chemical Industry Co. Ltd. were used in this work, see *Table 1*. This impact modifier is a complex chemical product that basically consists of a butadiene-based rubber core and a hard grafted methyl methacrylate copolymer shell; physical characterisation of this material has been described elsewhere[14].

All materials were predried for 16 hours at 80°C in a vacuum oven before melt processing. A Killion single screw extruder ($L/D = 30$, $D = 2.54$ cm) outfitted with an intensive mixing screw and a Baker-Perkins co-rotating, fully intermeshing twin screw extruder ($D = 15$ mm) were used for melt blending. For twin screw extrusion, the polycarbonate had to be fed in flake form. When flakes were not available from the supplier, pellets were cryo-ground to produce an acceptably small particulate size for feeding to the small twin screw extruder. Blends were extruded at 290°C and 40 rev min^{-1} in the single screw extruder (SS) and at 260 and 290°C at 160 rev min^{-1} in the twin screw extruder (TS).

The blends were injection moulded into Izod bars (ASTM D256) that were either 3.13 or 6.25 mm thick (see *Figure 1*) using an Arburg Allrounder injection moulding machine set at a melt temperature of 280°C and a mould temperature of 65°C. Specimens without defects were selected for testing.

Specimen geometry and Dynatup SN3PB configuration

Figure 1 shows the specimen geometry tested in the single-notch, three-point-bend configuration (SN3PB) using an instrumented Dynatup Drop Tower Model 8200 (see *Figure 2*). The guide slit (0.25 mm) was induced by a circular saw and the sharp notch was produced by tapping a fresh razor blade cooled in liquid nitrogen. All tests were made by dropping a 10 kg weight at a speed of 3.5 m sec^{-1} which is the same as that specified in the standard Izod test. During the test, a load cell in the tup measures the force generated within the deformed specimen at constant intervals while hammer speed is measured at the point of contact with the specimen. Assuming that the hammer does not change speed significantly due to the energy absorbed by the specimen and the effects of gravity during the fracture, the load–deflection curve can be obtained from the load–time curve. The integral of the load–deflection curve gives the energy absorbed by the specimen during fracture. Load–deflection curves and ductile–brittle transition temperatures were measured for a constant ligament size (10 mm).

Signal conditioning

Before comparison of the load–deflection curves, it is useful to eliminate or reduce the high frequency vibration components, i.e., 'ringing', received by the load cell. The process for reduction of this noise is shown schematically in *Figure 3*. Load waves obtained by the instrumented impact testing machine as a function of time (*Figure 3a*) were converted to amplitudes as a function of frequency by discrete Fourier transform analysis[38]. Fourier's theorem states that a function, x_i, may be expanded over the time range T as a series of the form

$$\begin{aligned} x_i &= \text{dc term} + \text{cosine term} + \text{sine term} \\ &= \frac{a_0}{2} + \sum_{n=1}^{N/2} a_n \cos\frac{2\pi nih}{T} + \sum_{n=1}^{N/2} b_n \sin\frac{2\pi nih}{T} \\ &= \sum_{n=0}^{N/2} a_n \cos\frac{2\pi in}{N} + \sum_{n=0}^{N/2} b_n \sin\frac{2\pi in}{N} \end{aligned} \quad (1)$$

In equation (1), N is the number of data points, h is sampling interval while a_n and b_n are Fourier coefficients.

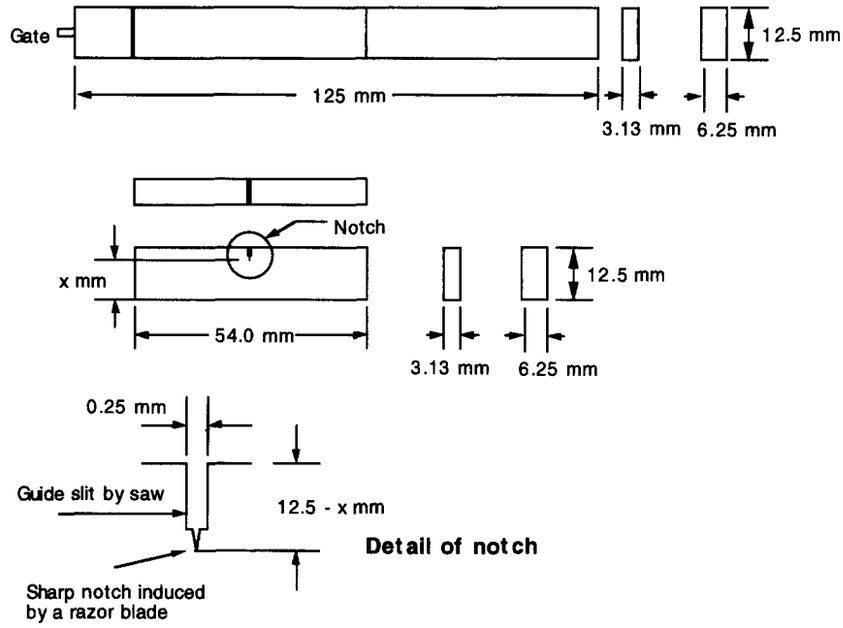

Figure 1 Specimen geometry used in single-notch, three-point-bend, SN3PB, impact testing by Dynatup

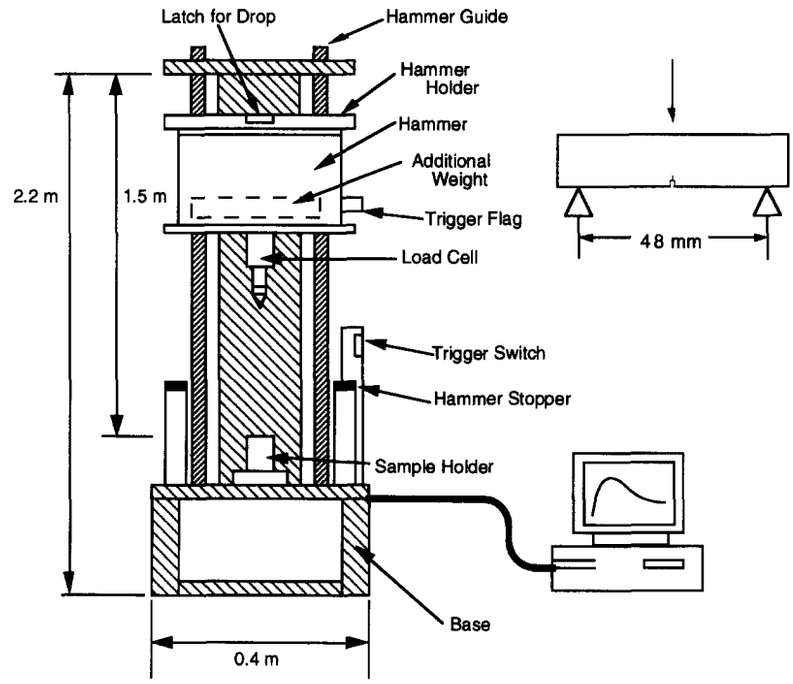

Figure 2 Schematic of Dynatup impact test apparatus

The coefficients are defined by the following equations

$$\frac{a_0}{2} = \frac{1}{N}\sum_{i=1}^{N} x_i \tag{2}$$

$$a_n = \frac{N}{2}\sum_{i=1}^{n} x_i \cos\frac{2\pi in}{N} \tag{3}$$

$$b_n = \frac{N}{2}\sum_{i=1}^{n} x_i \sin\frac{2\pi in}{N} \tag{4}$$

where $n = 1, 2, 3, \ldots, N/2$.

Since both coefficient sets represent the same frequency, ω, they can be combined into a single vector sum to represent the modulus and phase of each of the harmonic amplitudes

$$C_n = \sqrt{a_n^2 + b_n^2} \tag{5}$$

$$\theta_n = \arctan\frac{b_n}{a_n} \tag{6}$$

After Fourier transformation, each harmonic amplitude

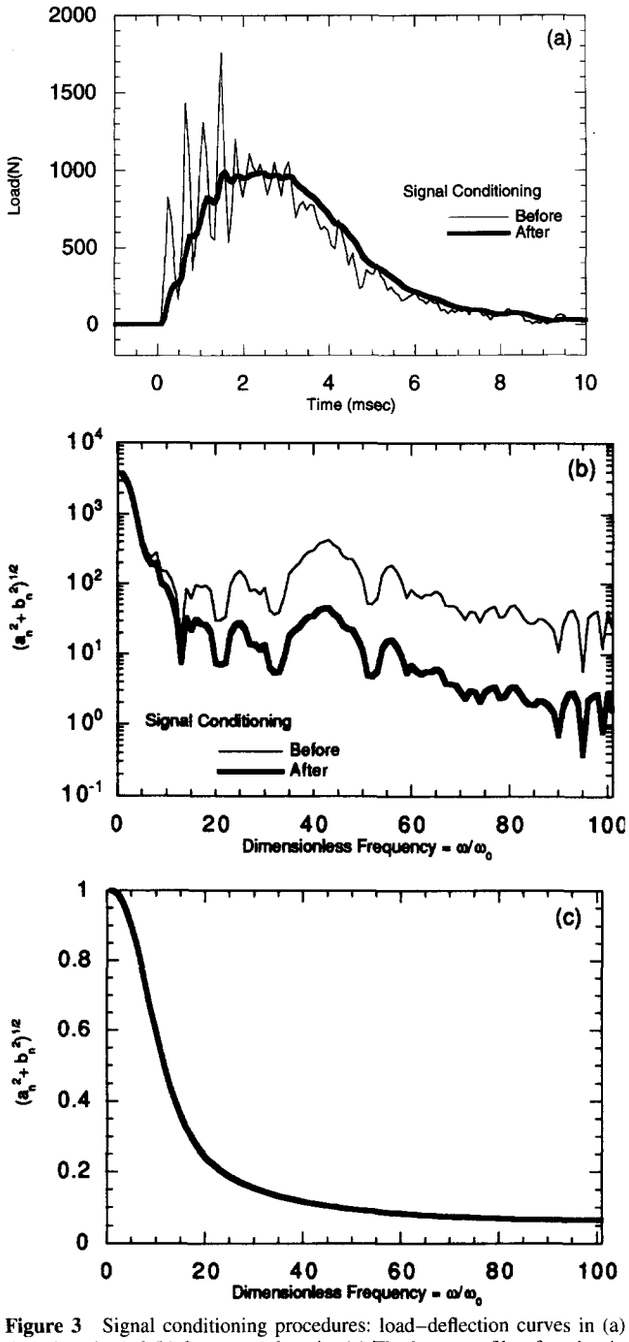

Figure 3 Signal conditioning procedures: load–deflection curves in (a) time domain and (b) frequency domain. (c) The low pass filter function in frequency domain

is shown as a function of harmonics of the fundamental frequency, $\omega_0 = 2\pi/(Nh)$. Original and conditioned waves are shown in *Figure 3a*. Original load–time curves were transformed to a frequency domain by using Fourier's theorem described above. *Figure 3b* shows $\sqrt{a_n^2 + b_n^2}$ as a function of dimensionless frequency, i.e., the power spectrum of the waves. In the frequency domain, higher frequency components were eliminated by using the digital low pass filter shown in *Figure 3c* as the power spectrum. High frequency components were reduced as shown in *Figure 3b*. By using proper low pass filters, noise components can be eliminated or reduced from the original wave without changing the characteristic features of the wave (*Figure 3a*). After signal conditioning, load–time curves were transformed to load–deflection curves by assuming constant hammer speed as previously described. All impact load–deflection curves shown in this report have been conditioned as described above.

TEM observation of fracture

Transmission electron microscopy (TEM) was used to observe the deformation around the tip of arrested cracks. These arrested cracks were generated in 6.25 mm thick specimens with a 10 mm ligament size using the technique shown in *Figure 4*. Crack extension was arrested at the mid-point of the original ligament by adjusting the height of the hammer stoppers. These partially fractured specimens were embedded in epoxy resin (Araldite 502) to avoid further deformation during preparation for microtoming. A block containing the crack was cut from the specimen by a milling machine and a fresh razor blade. The observation plane was selected from the centre of the thickness direction and parallel to both the injection flow and the crack extension directions. After making a mesa-cut, thin sections (15–20 nm) were prepared by a Reichert–Jung Ultracut E microtome under cryogenic conditions (−45°C) with a diamond knife. Thin sections were stained by exposure to vapours of a 2% osmium tetroxide (OsO_4) solution for 18 hours at room temperature. The butadiene-based rubber core appears black in the TEM images. Photomicrographs were made sequentially from the crack tip to the undeformed region using a JEOL 200 CX transmission electron microscope at an accelerating voltage of 120 kV. TEM observations were made under both bright and dark field conditions to obtain a better understanding of where voids had formed inside rubber particles.

IMPACT LOAD CURVE ANALYSIS

Figure 5 shows impact load–deflection curves obtained at 24°C for pure PC and blends containing 6% impact modifier prepared by different compounding procedures. Blends prepared in the twin screw extruder show typical curves of stable crack propagation in ductile fracture. Clearly, much more energy is absorbed during fracture by these blends than by neat PC or blends of the same composition prepared in a single screw extruder. The latter show brittle behaviour regardless of the molecular weight of the PC matrix (*Figure 5a* and *b*). The tough blends made in the twin screw extruder undergo more deflection before total fracture of the ligament when the PC matrix molecular weight is higher. Previous work[14] has shown that the impact modifier is significantly better dispersed in all PC blends made in the twin screw extruder in comparison to those made in the single screw extruder.

Figure 6 shows load–deflection curves at 24°C for blends based on the medium molecular weight grade of PC containing various concentrations of the core–shell impact modifier prepared by a single pass through the twin screw extruder at 260°C. Blends containing 6% or more modifier show ductile fracture while the blend containing 3% modifier shows brittle fracture. The initial slopes of the load versus deflection curves for the blends containing 3% and 6% modifier are slightly higher than for the blends containing 12% and 18% modifier. This agrees with the previous observation that the tensile modulus of blends based on M-PC prepared in the twin screw extruder is hardly affected by addition of up to 6% impact modifier but decreases at higher concentration[14]. The blend containing 6% modifier shows the highest maximum load of the compositions shown in *Figure 6*.

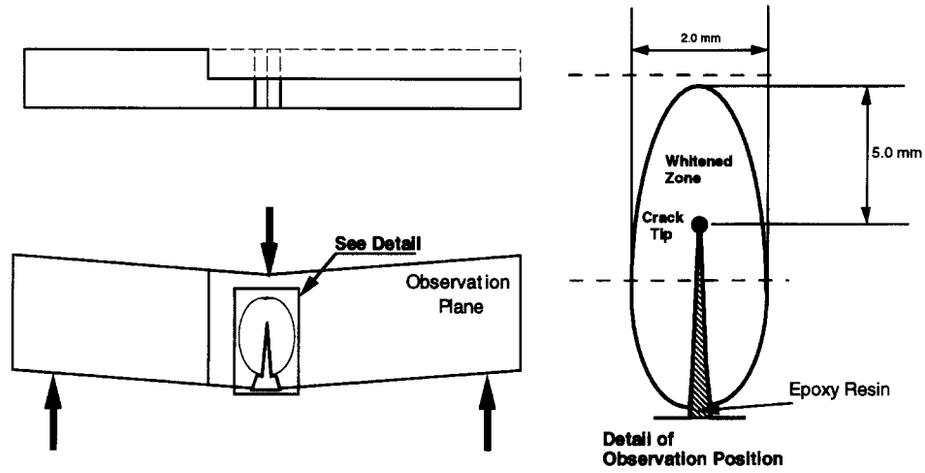

Figure 4 Schematic of arrested crack specimen for TEM observation

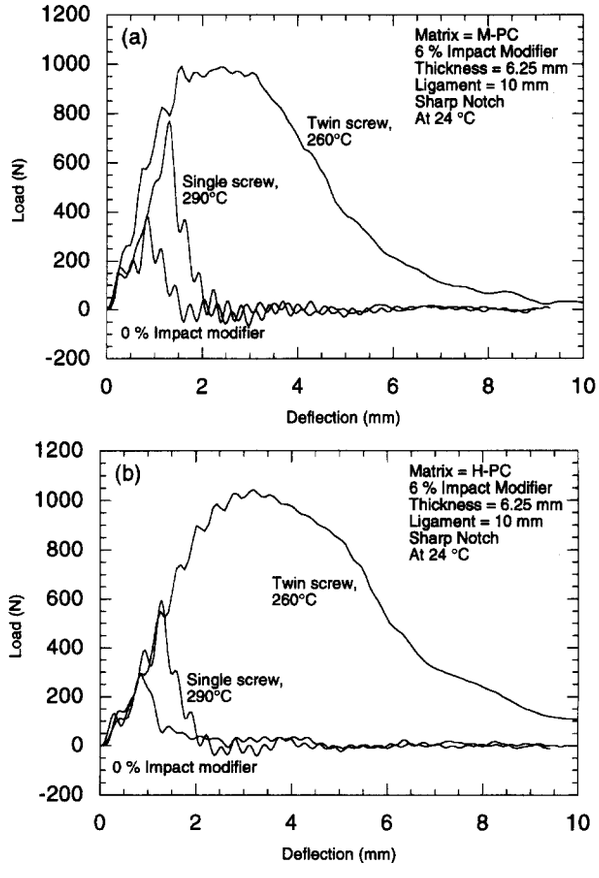

Figure 5 Impact load–deflection curves at 24°C for PC/6% modifier blends prepared by different procedures: (a) M-PC matrix and (b) H-PC matrix

Figure 7 compares load–deflection curves at 24°C for thick and thin specimens of PC/modifier blends (94/6) where the load has been normalised by specimen thickness. There are slight differences when the matrix is M-PC (*Figure 7a*) while essentially identical normalised curves are seen when the matrix is H-PC (*Figure 7b*). Thus, PC blends containing 6% of this impact modifier have essentially identical fracture properties, independent of specimen thickness, in this range of thickness and for these test conditions.

IMPACT TOUGHNESS AS A FUNCTION OF TEMPERATURE FOR THICK SPECIMENS WITH A SHARP NOTCH

Values of impact fracture energy for 6.25 mm thick specimens with a sharp notch and a ligament length of 10 mm were calculated by integrating the load–deflection curves without signal conditioning. The results are plotted as a function of test temperature in *Figures 8 and 9* and summarised in *Table 2*. The Dynatup impact strength at room temperature for the thick specimens that fail in a ductile manner tends to be slightly higher than values from a standard notched Izod test using 3.13 mm thick specimens. Generally, thicker specimens with a sharp notch show less impact strength; however, the current reversal may be attributed to differences in the sample configuration of the Izod test (cantilever bending) versus that used here in the Dynatup (three point bending). The fracture mode in Izod impact testing of very ductile materials usually leads to partial breaks that leave a rather large unbroken ligament because the specimens deflect out of the path of the hammer; while in the Dynatup test used here, the breaks are more likely to be complete but when hinged breaks do occur there is very little unbroken ligament since it more difficult in three point bending for the specimen to deflect out of the path of the hammer. PC/modifier blends described here do not show significant differences in fracture energy between specimens taken from the gate end and from the far end of the moulded bar. Each data point represents an average of at least four specimens from both the gate and far ends. Both neat M-PC and H-PC were found to be brittle at all testing temperatures. *Figure 8* shows the results for blends containing 6% modifier prepared in different ways. Blends prepared in the twin screw extruder at 260°C have the highest fracture energy at room temperature and the lowest ductile–brittle temperature, 10°C for blends based on M-PC (*Figure 8a*) and 5°C for blends based on H-PC (*Figure 8b*) for all process conditions. Blends prepared in the single screw extruder based on H-PC show ductile fracture above 40°C while corresponding blends based on M-PC were brittle at all testing temperatures.

The effect of core–shell modifier concentration on impact strength as a function of temperature is shown in *Figure 9*. For blends prepared in the single screw extruder, *Figure 9a* shows that increasing the impact modifier concentration slightly increases room temperature impact strength, but all blends fracture in a brittle manner at 24°C. Some reduction

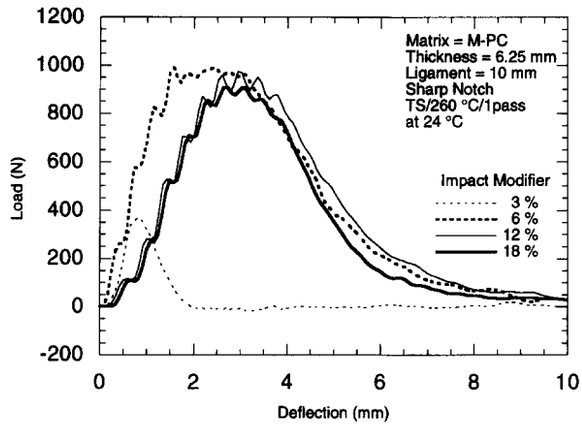

Figure 6 Impact load–deflection curves at 24°C for blends of M-PC with various concentrations of core–shell modifier prepared in the twin screw extruder

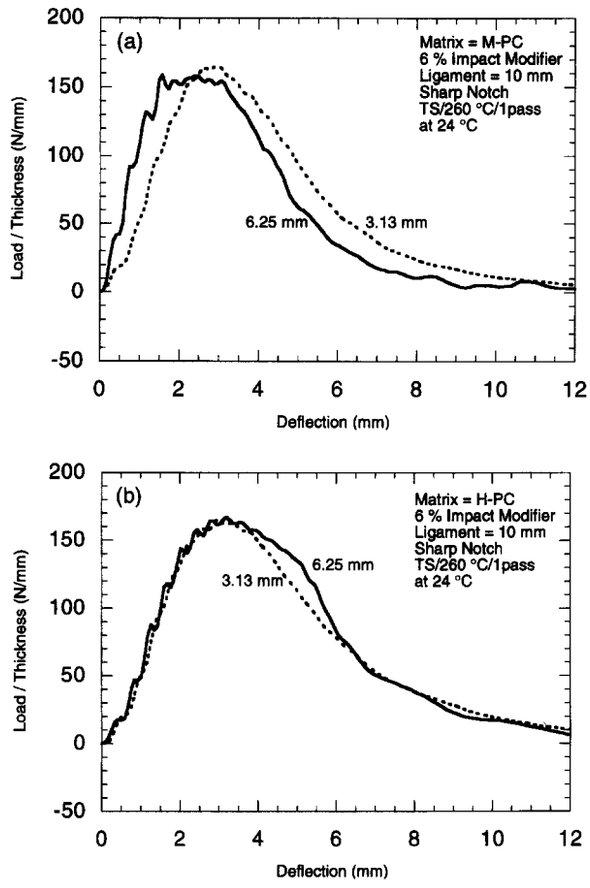

Figure 7 Impact load–deflection curves at 24°C for thick and thin specimens of PC/6% modifier blends based on (a) M-PC and (b) H-PC prepared in the twin screw extruder

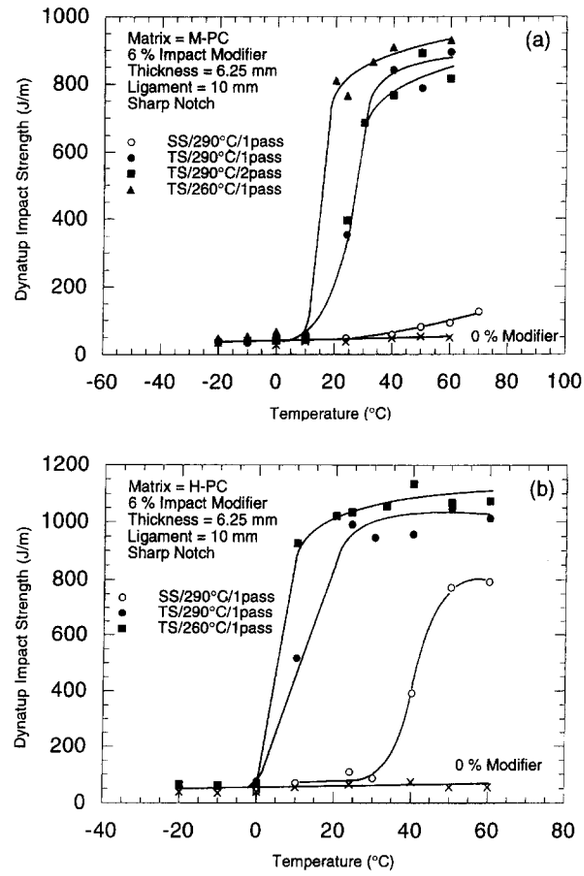

Figure 8 Dynatup impact toughness of PC/6% modifier blends prepared by different procedures using thick specimens with a sharp notch: (a) M-PC matrix and (b) H-PC matrix

of the ductile–brittle transition temperature is observed. Blends prepared in the twin screw extruder that contain more than 6% or more modifier are tough at room temperature, i.e., the ductile–brittle transition temperature is below room temperature (*Figure 9b*). Concentrations of modifier above 6% decrease room temperature toughness but give lower ductile–brittle transition temperatures; the blends containing 12% and 18% modifier have a ductile–brittle transition temperature of −15°C.

Blends with good dispersion of the impact modifier as prepared in the twin screw extruder have superior impact properties when specimens are thick and have a sharp notch compared to neat PC or blends made in the single screw extruder.

The previous paper[14] showed that addition of the core–shell impact modifier to polycarbonate does not improve the room temperature toughness of thin specimens (3.13 mm thick) with a standard notch regardless of modifier concentration, process conditions, or molecular weight of the PC matrix. However, blends where the modifier is better dispersed showed less decrease in toughness and had lower ductile–brittle transition temperatures. Of course, thin specimens of neat PC are ductile at room temperature and have a low ductile–brittle transition temperature (−10 to −45°C). Addition of the modifier leads to less energy absorption at room temperature and a rather similar ductile–brittle transition temperature even when the modifier is well dispersed in the PC matrix. Poor dispersion of the impact modifier particles significantly reduces room temperature toughness and leads to much higher transition temperatures in comparison to neat PC. The Dynatup impact test using thick specimens with a sharp notch shows a more clear discrimination of the toughening effect caused by impact modifier at different concentrations and degrees of dispersion. Blends containing more than 6% modifier that is well dispersed show dramatic improvement in toughness compared to neat PC, while blends having poor dispersion of the modifier do not show any improvement. These blends are tough like thin neat PC specimens and have ductile–brittle transition temperatures

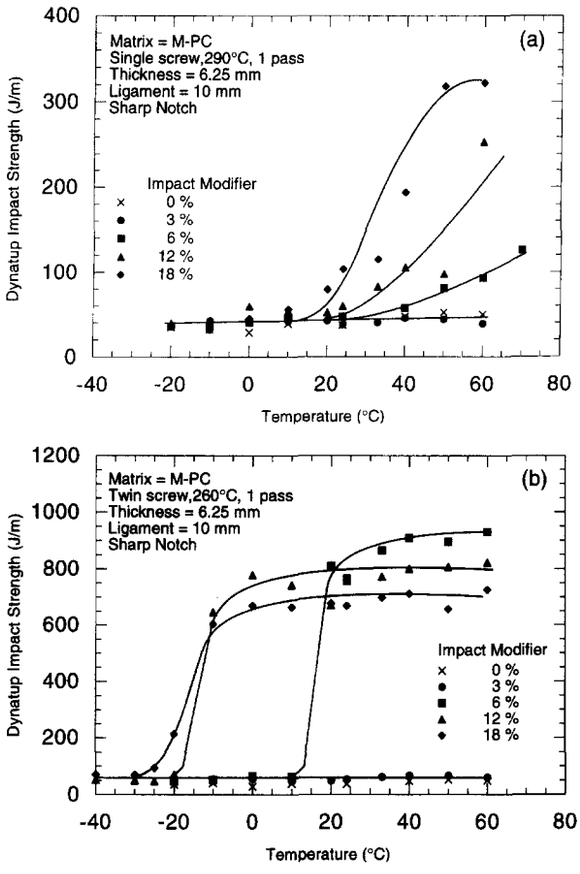

Figure 9 Dynatup impact strength of blends based on M-PC containing various concentrations of core–shell modifier prepared in (a) the single screw extruder and (b) the twin screw extruder for thick specimens with a sharp notch

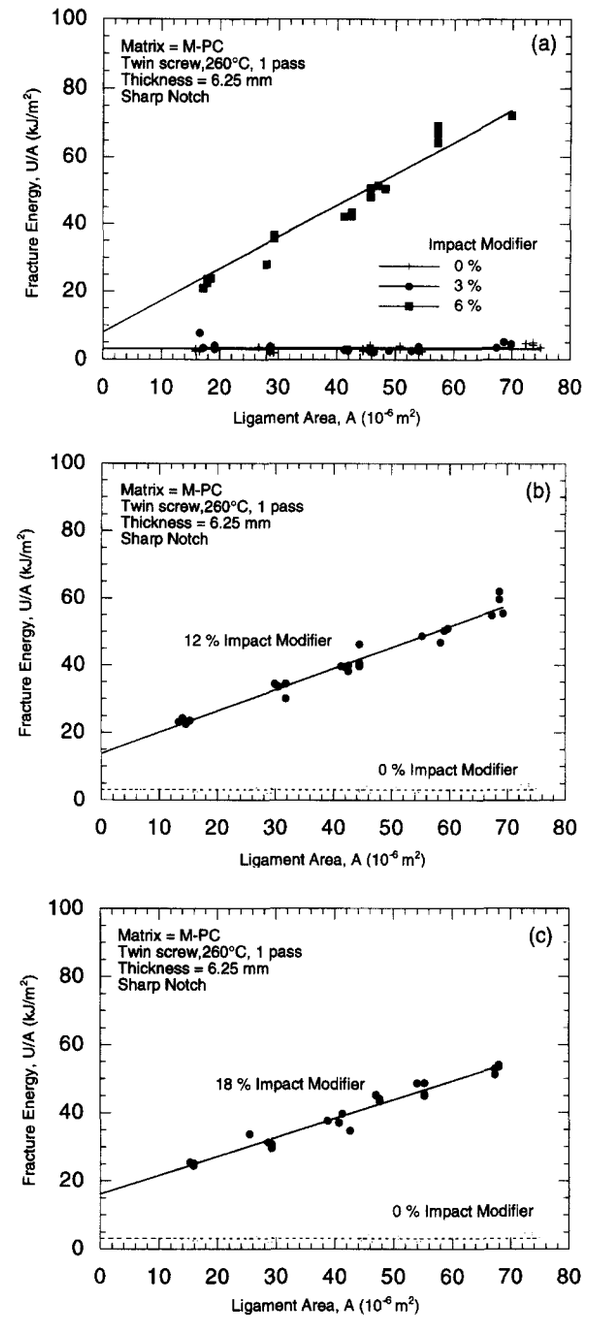

Figure 10 Fracture energy as a function of ligament area for M-PC blends prepared in the twin screw extruder using thick specimens with a sharp notch containing: (a) 0, 3 and 6%; (b) 12%; (c) 18% of the core–shell modifier

below room temperature, while neat PC shows brittle fracture over the entire temperature range used here.

Vu-Khanh analysis

As mentioned earlier, Vu-Khanh[24] has shown that considerably greater insight about the fracture toughness of ductile plastics can be gained from analysis of the fracture energy as a function of the ligament area. Vu-Khanh showed that the fracture energy per unit of ligament area, U/A, is a linear function of the ligament area A. He defined two parameters by the relationship

$$\frac{U}{A} = G_i + \frac{1}{2}T_a A \tag{7}$$

The quantity G_i has been termed the fracture energy at initiation, while T_a has been interpreted as the tearing modulus. Vu-Khanh showed evidence for toughened nylon 66 (Zytel ST-801 from Du Pont) and a PC/polyethylene blend that the fracture energies at initiation, G_i, obtained by this method at low strain rate are similar in magnitude to the J_{IC} values for these materials. Recently, Crouch and Huang have also shown that the resistance curve (J–R curve) has a low dependence on testing rate[18]. The two Vu-Khanh parameters can be very useful for characterising the toughness of ductile materials even though there is some controversy about their physical meaning[34]. Such an analysis was applied at room temperature for the blends described above.

Figure 10 shows sample plots of fracture energy (U/A) as a function of a ligament area for blends of the medium molecular weight grade of polycarbonate, M-PC, with different concentrations of impact modifier prepared by a single pass through the twin screw extruder at 260°C. The data for each material show a relatively good linear relationship between the fracture energy and the ligament area. From such plots, the two parameters in equation (7) were determined from the intercept and the slope. *Figure 11* shows the fracture energy at initiation, G_i, and the tearing modulus, T_a, as a function of modifier concentration for blends based on M-PC prepared by two different procedures: one pass through the twin screw extruder at 260°C (TS/260°C/1 pass) or the single extruder at 290°C (SS/290°C/1 pass). The neat polycarbonate shows a low value of the intercept, G_i, and a zero slope, $T_a = 0$,

Table 2 Summary of impact strength characterisation

		Extrusion conditions			Notched Izod impact strength of 3.13 mm specimens with standard notch		Dynatup impact strength of 6.25 mm specimens with sharp notch		Vu-Khanh parameters	
Matrix PC	Impact modifier content (wt%)	Extruder type	No. of passes	Process temp. (°C)	Impact strength ($J\ m^{-1}$)	Ductile–brittle transition temperature (°C)	Impact strength ($J\ m^{-1}$)	Ductile–brittle transition temperature (°C)	Fracture energy at initiation G_i ($kJ\ m^{-2}$)	Tearing modulus T ($10^6\ kJ\ m^{-4}$)
M-PC	0	N/A	N/A	N/A	874	−35	37	> 60	3.2	0.0
H-PC	0	N/A	N/A	N/A	991	−45	65	> 60	4.1	0.0
M-PC	3	Single	1	290	697	+ 10	38	> 60	3.3	0.0
		Twin	1	260	834	−35	54	> 60	3.5	0.0
	6	Single	1	290	622	+ 10	47	> 60	4.2	0.0
		Twin	1	290	770	−30	354	20	6.9	1.8
			2	290	710	−30	395	20	9.9	1.3
			1	260	818	−35	765	10	8.0	1.9
	12	Single	1	290	488	+ 10	60	60	4.6	0.0
		Twin	1	260	656	−55	758	−15	13.9	1.2
	18	Single	1	290	362	+ 10	103	40	8.6	0.0
		Twin	1	260	585	−40	668	−20	16.3	1.1
H-PC	6	Single	1	290	683	−15	109	40	5.5	0.0
		Twin	1	290	831	−45	992	5	8.0	2.2
				260	881	−35	1035	5	9.2	2.5

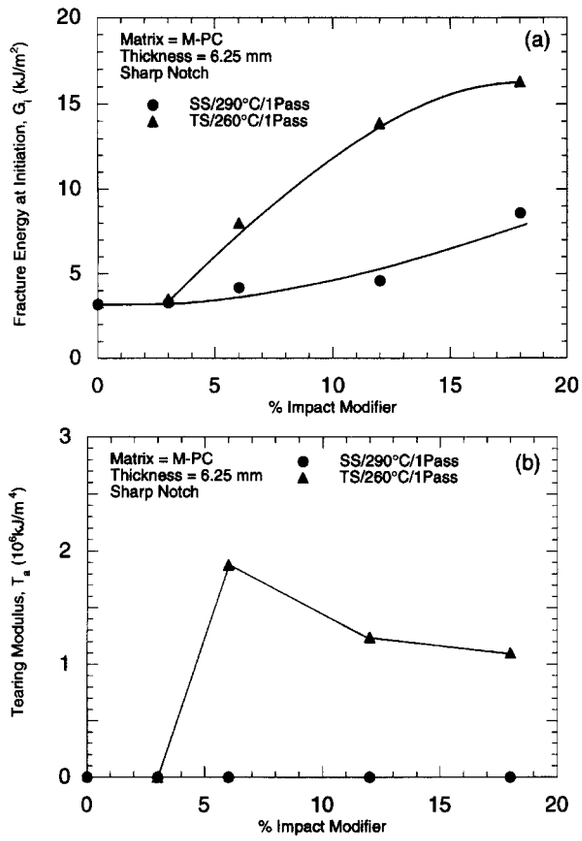

Figure 11 Fracture energy at initiation (a) and tearing modulus (b) as a function of impact modifier concentration for M-PC blend prepared in the single and the twin screw extruder using thick specimens with a sharp notch

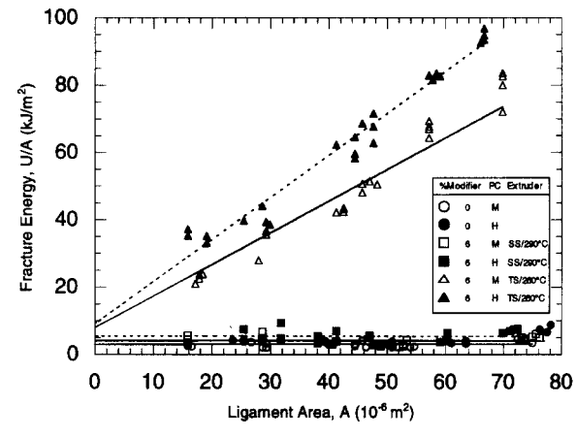

Figure 12 Fracture energy as a function of ligament area for neat PC and PC/6% modifier blends based on M-PC and H-PC prepared by different procedures using thick specimens with a sharp notch

indicative of its brittle nature under plane strain conditions, i.e., thick specimens with a sharp notch. Addition of impact modifier improves the fracture energy at initiation in all cases, but the better dispersion produced by the twin screw extruder clearly leads to more dramatic improvements than achieved by blending in the single screw extruder. Blends prepared in the single screw extruder show zero slope or tearing modulus regardless of the amount of impact modifier added. However, when the impact modifier is rather well dispersed by use of the twin screw extruder, there are substantial increases in the fracture energy at initiation, G_i, and in the tearing modulus, T_a, when the impact modifier

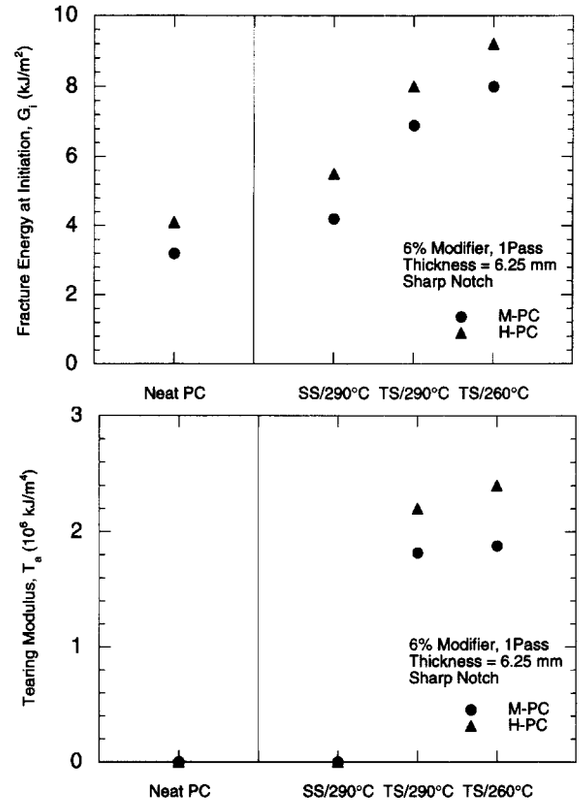

Figure 13 Fracture energy at initiation (a) and tearing modulus (b) as a function of process conditions for neat PC and PC/6% modifier blends based on M-PC and H-PC using thick specimens with a sharp notch

concentration is 6% by weight or more. The tearing modulus appears to be greatest at 6% modifier while the fracture energy at initiation continues to increase with further modifier addition. The benefit of this detailed analysis in comparison to Izod or Charpy type testing is to differentiate to what extent the increase in energy to produce a complete fracture stems from changes in the fracture energy at initiation, G_i, and/or the changes in the tearing modulus, T_a. The parameters G_i and T_a can in principle be related to specific performance requirements of materials; however, it is not yet clear how effectively the two parameters can be varied independently by formulation.

Similar analyses were made for a fixed impact modifier content of 6% to examine the effects of polycarbonate molecular weight and blend compounding conditions, see *Figure 12*. The neat polycarbonate and blends prepared in the single screw extruder all show brittle behaviour while all blends prepared in the twin screw extruder show very ductile behaviour. The fracture energy at initiation for neat polycarbonate is slightly higher for the higher molecular weight grade; however, the tearing modulus is zero for both grades. The values of G_i obtained for neat PC, 3.2 kJ m^{-2} for M-PC and 4.1 kJ m^{-2}, are similar to the value of J_{IC} = 4.8 kJ m^{-2} obtained by Plati and Williams using the usual measurement method[46]. For both PC grades, addition of impact modifier increases the fracture energy at initiation; the effect is greater for processing procedures that improve the degree of dispersion of the modifier[14] as seen in *Figure 13a*. The tearing modulus is much more sensitive to the degree of dispersion of the impact modifier. Only blends prepared in the twin screw extruder show finite values of tearing modulus; blends based on H-PC show slightly higher values than those based on M-PC.

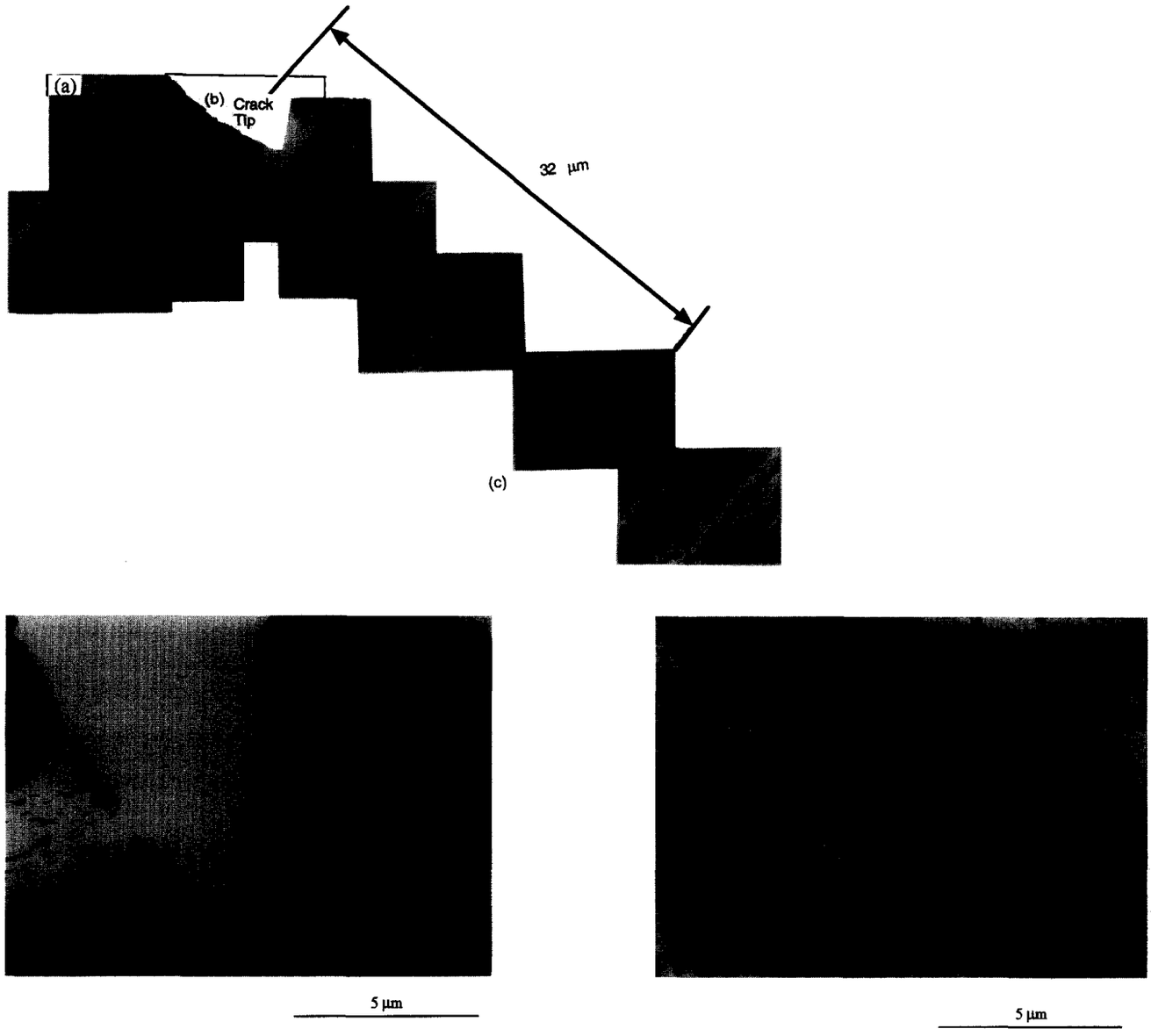

Figure 14 Electron photomicrographs showing the morphology of the deformed zone in the vicinity of the arrested crack tip for an M-PC blend containing 6% modifier prepared in the twin screw extruder: (a) a composite of views showing region ahead of crack tip, (b) expanded view of crack tip, (c) expanded view of area 32 μm ahead of crack tip

TEM OBSERVATION OF REGION AROUND AN ARRESTED CRACK

In order to understand the deformation processes that occur in these impact modified PC blends, cracks formed during high speed testing of 6.25 mm thick specimens with sharp notches were arrested and the surrounding region was examined by TEM using the techniques described earlier. An example is shown in *Figure 14* for a tough blend based on M-PC containing 6% impact modifier prepared in the twin screw extruder at 260°C. *Figure 14a* is a composite of several photomicrographs that show the region near and well forward of the arrested crack tip. More detailed views of the regions defined by the rectangles are shown in *Figure 14b* and *c*. Near the crack tip or its surfaces, the impact modifier particles are elongated in the direction perpendicular to the crack propagation evidently due to matrix shear yielding. These events appear to blunt the sharpness of the crack tip (*Figure 14b*). Well ahead of the crack tip, many of the core–shell particles were found to have cavitated (*Figure 14c*). High magnification TEM microphotographs of this region are shown under bright field (*Figure 15a*) and dark field (*Figure 15b*) conditions; holes appear as white spots in the bright field while they appear as black spots in the dark field. All the white spots seen in the bright field do not appear as black spots in the dark field. A potential explanation of this is suggested in *Figure 16*. The microtomed sections, are thin, 15–20 nm, compared to the diameter of the core–shell impact modifier particles, typically 60–150 nm. Thus, the microtome cut may transverse a cavity that does not go all the way through the section. In the bright field these particles will show lighter regions than particles that are not cavitated but will not necessarily appear as black spots in the dark field. In any case, the black spots in the dark field represent definitive evidence of cavitation in some of the particles, while the above interpretation of the bright field views suggests that cavitation is even more extensive than shown in dark field. These results suggest that a large region of the matrix is able to yield after the core–shell particles cavitate ahead of the

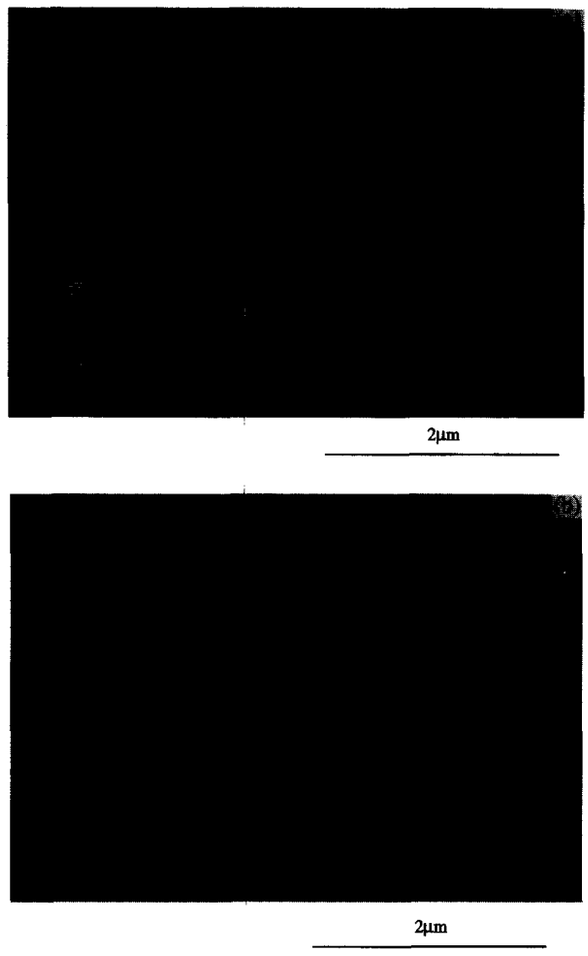

Figure 15 High magnification TEM photomicrographs under (a) bright field and (b) dark field conditions for a M-PC/6% modifier blend prepared in the twin screw extruder in the region ahead of crack tip where particle cavitation occurs

crack tip. According to this interpretation, there is a triaxial stress state well ahead of the crack tip which prevents matrix yielding but does lead to rubber cavitation; cavitation of rubber relieves this triaxial stress or plane strain condition and allows the matrix to yield. Evidently good dispersion of the impact modifier is required for these particles to cavitate since no cavitation could be found in the brittle blends that have poor modifier dispersion. This is illustrated in *Figure 17a* and *b* which show the deformed morphology near the crack surface for blends based on M-PC containing 6% modifier. The blend prepared in the twin screw extruder, which leads to good dispersion of modifier particles, shows extensive shear yielding and cavitation of particles (*Figure 17a*) while a corresponding blend prepared in the single screw extruder, which leads to poorer dispersion, does not show any cavitation (*Figure 17b*). Aggregation of impact modifier particles of fixed size and concentration leads to larger regions of matrix that contain no modifier, i.e., interparticle distance is increased. This appears to be deleterious for toughening of polycarbonate; several factors may be responsible. Recent literature has stressed the importance of cooperativity among adjacent particles in the cavitation process[8–11]. This is likely to be strongly influenced by how close the particles are to each other since this cooperativity must involve interaction of stress fields around adjacent particles. In addition, the actual particle size, independent of distance between particles, may play a role when cavitation is involved[44]. Of course, in the present case these are actually aggregates or clusters of individual core–shell emulsion particles whose propensity for cavitation may be quite different than a single core–shell particle of the same diameter as the cluster.

TOUGHENING MECHANISM OF PC/CORE–SHELL MODIFIER BLENDS

The Izod impact strength of PC/modifier blends obtained using relatively thin, i.e., 3.13 mm, specimens with a standard notch is less than that of neat PC which is already very tough under these fracture conditions, regardless of compounding method, modifier concentration and PC molecular weight; however, for 6.25 mm thick specimens with a sharp notch there is dramatic improvement on adding modifier relative to pure PC which is brittle under these fracture conditions. From the above TEM observations around the tip of the arrested crack formed under high speed loading, cavitation of modifier particles appears to induce matrix yielding ahead of the crack[11,39–41]. According to current models, as mentioned above, the role of particle cavitation is to relieve the triaxial stress, i.e., inducing a transition from a plane strain condition to a plane stress condition around the crack tip. For this mechanism to be effective, the region of particle cavitation under plane strain conditions must be much larger than the original yield region that would exist without modifier particles. Once enough particle cavitation has occurred to relieve the triaxial stress, the yield region will extend. The toughening effect caused by particle cavitation would be less important under plane stress conditions. In this situation, the particle cavitation process contributes positive effects like local yielding around particles plus crack blunting and branching but these may be outweighed by deleterious effects like the decrease in yield stress and crack extension by connecting the voids. Thus, under the moderate conditions of an Izod test employing thin specimens with a standard notch, addition of modifier to PC may not improve impact strength of the already tough matrix.

As suggested above, a key issue in whether toughening occurs in plane stress or plane strain conditions is the relative size of the yield zone in the absence of modifier versus the size of the cavitation zone when modifier particles are present. Simple model calculations in the vicinity of a crack

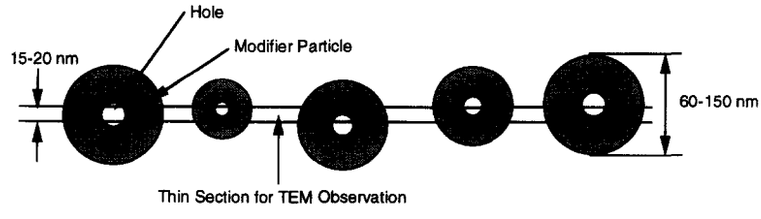

Figure 16 Schematic showing the microtomed thin section cut from the cavitated region for TEM observation

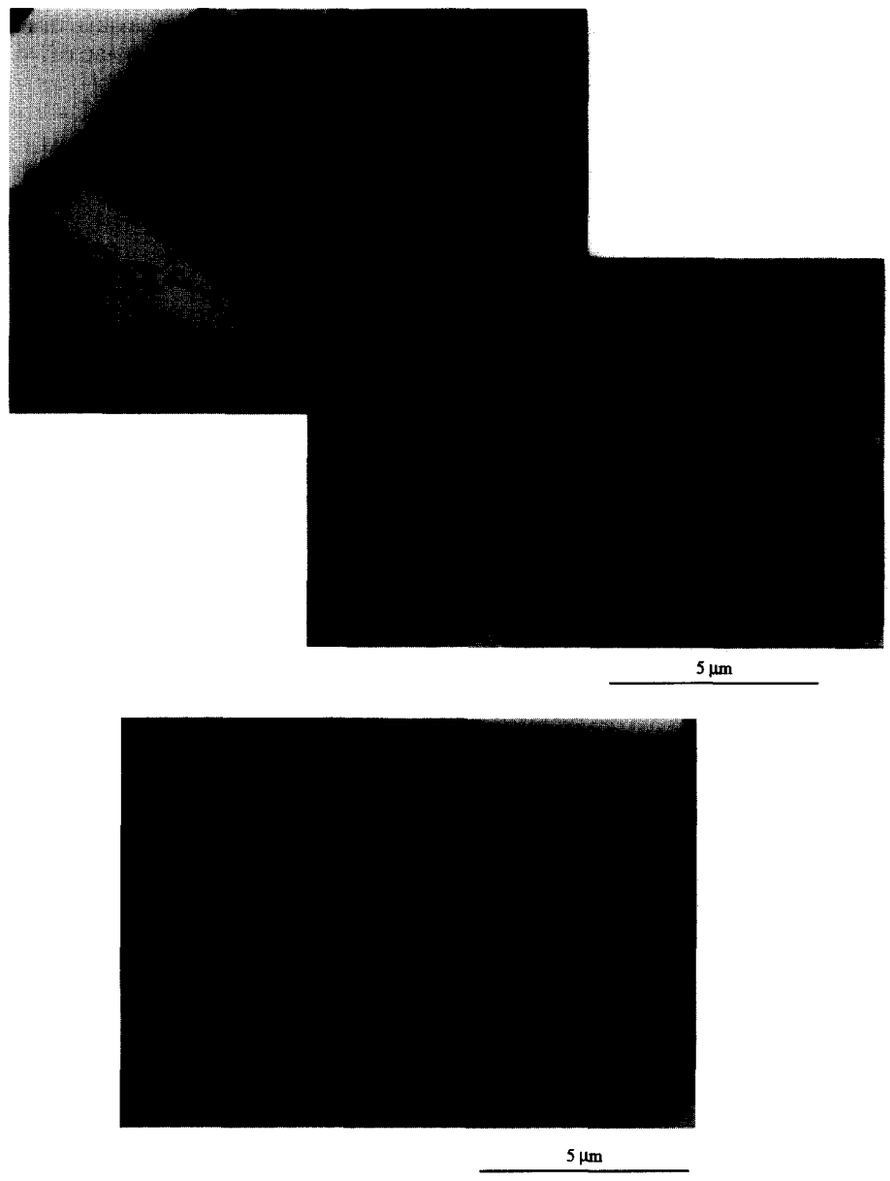

Figure 17 Morphology of deformed zone beneath the crack surface of M-PC/6% modifier blends prepared in (a) the twin screw extruder at 260°C and (b) the single screw extruder at 290°C

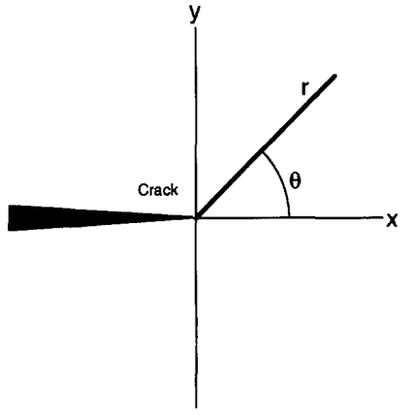

Figure 18 Coordinates around a sharp crack

tip were performed to estimate the size of the yield and cavitation regions under both plane stress and plane strain conditions. According to linear elastic fracture mechanics, the principal stresses at distance r from a sharp crack and angle Θ from the direction of crack propagation (*Figure 18*) are given by the following equations[42]

$$\sigma_1 = \frac{K_{IC}\cos\left(\frac{\theta}{2}\right)\left(1+\sin\left(\frac{\theta}{2}\right)\right)}{\sqrt{2\pi \cdot r}} \tag{8}$$

$$\sigma_2 = \frac{K_{IC}\cos\left(\frac{\theta}{2}\right)\left(1-\sin\left(\frac{\theta}{2}\right)\right)}{\sqrt{2\pi \cdot r}} \tag{9}$$

$$\text{for plane strain } \sigma_3 = \frac{2\nu \cdot K_{IC}\cos\left(\frac{\theta}{2}\right)}{\sqrt{2\pi \cdot r}} \tag{10}$$

$$\text{for plane stress } \sigma_3 = 0$$

where K_{IC} is the critical stress intensity factor and ν is Poisson's ratio. Strain components can be expressed in

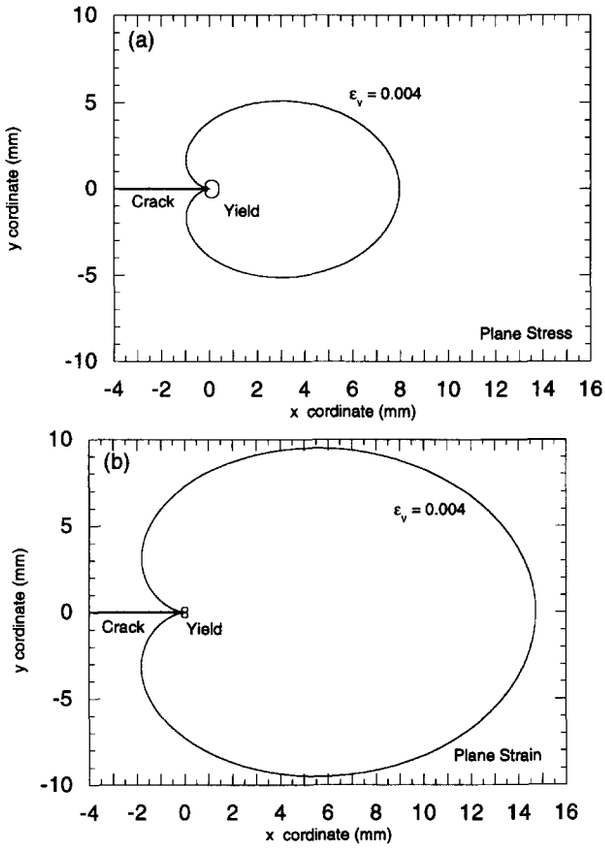

Figure 19 Calculated yield zone and region where 0.4% volumetric strain is achieved under (a) plane stress and (b) plane strain conditions

terms of the principal stress components as follows

$$\varepsilon_1 = \frac{1}{E}(\sigma_1 - \nu(\sigma_2 - \sigma_3)) \tag{11}$$

$$\varepsilon_2 = \frac{1}{E}(\sigma_2 - \nu(\sigma_3 - \sigma_1)) \tag{12}$$

$$\varepsilon_3 = \frac{1}{E}(\sigma_3 - \nu(\sigma_1 - \sigma_2)) \tag{13}$$

where E is the tensile modulus. The cavitation region may be defined by assuming that cavitation occurs when the volumetric strain, ε_v, exceeds some critical value, ε_{vc}, i.e.

$$\varepsilon_v = (1+\varepsilon_1)(1+\varepsilon_2)(1+\varepsilon_3) - 1 > \varepsilon_{vc} \tag{14}$$

Bucknall[43,44] has suggested ε_{vc} is about 0.4% for natural rubber. In these model calculations, we assume that a 0.4% volumetric strain causes cavitation since no other criterion for the rubber core of the currently used impact modifier is available, and we use the following material constants which were obtained under static loading conditions: $E = 2.0\,\text{GPa}$[14]; $\sigma_y = 6\,\text{MPa}$[14]; $K_{IC} = 3\,\text{MN/m}^{-1/2}$ [45] and $\upsilon = 0.35$ (estimated). The simple Von Mises yield criterion was used to determine the matrix yield region

$$(\sigma_1 - \sigma_2)^2 + (\sigma_2 - \sigma_3)^2 + (\sigma_3 - \sigma_1)^2 = 2\sigma_y^2 \tag{15}$$

ignoring effects of pressure or porosity since they make only very small changes in the size of the yield region[44].

Figure 19 shows the calculated regions near a sharp crack tip where yield and cavitation are expected based on the criterion outlined. As shown in *Figure 19*, the yield and cavitation regions are closer in size in plane stress than they are in plane strain. Thus, for plane stress condition or thin specimens, a higher fracture energy can result from yielding of the matrix itself without the aid of particle cavitation. On the other hand, for plane strain conditions or thick specimens, the yield region is much smaller while the cavitation region is much larger than in plane stress. In this case, a transition from plane strain to plane stress conditions caused by rubber cavitation can lead to a high fracture energy as the matrix is allowed to yield.

SUMMARY AND CONCLUSIONS

The impact fracture behaviour of PC/core–shell impact modifier blends in the form of thick specimens with sharp notches, prepared by different compounding processes was examined by a variety of techniques including the Vu-Khanh method of analysis. Impact testing using thick specimens with sharp notches give much better discrimination of the effects of adding such an impact modifier to PC, as seen by response to concentration and degree of dispersion of the impact modifier in PC matrix, than Izod testing using thin specimens with standard notches. Blends containing more than 6% modifier that is well dispersed show dramatically improved impact properties in thick specimens (6.25 mm) in comparison to neat PC, while blends having poor dispersion of the modifier do not show any improvement. In thick specimens, blends containing more than 6% modifier are tough like neat thin PC specimens and have ductile–brittle transition temperature below room temperature, while thick specimens of neat PC show brittle fracture over the range of test temperatures used.

Both parameters obtained from the Vu-Khanh analysis, i.e., the fracture energy at initiation, G_i, and the tearing modulus, T_a, increase as the concentration of modifier, the degree of dispersion of the modifier, and the PC molecular weight increase. The benefit of this analysis in comparison to Izod or Charpy type testing is to provide more information about how specimen geometry, or ligament size, affects fracture energy. In this context, the Izod or Charpy methods represent single point tests since only one ligament size is used. The fracture energy at initiation, G_i, and the tearing modulus, T_a, may be useful in the design of engineering thermoplastics alloys for specific applications. That is, for certain applications it may be important to have a large value of G_i while other situations may benefit more from a high value of T_a. In the current work it appears that factors which improve one of these parameters also tends to improve the other; however, it may be possible by more sophisticated formulation to influence these two characteristics of the fracture process somewhat independently.

TEM observations, model calculations based on linear fracture mechanics, and comparison of the fracture behaviour of thick versus thin specimens are all consistent with a toughening mechanism involving cavitation of modifier particles ahead of an advancing crack to relieve a triaxial stress state which permits matrix yielding.

ACKNOWLEDGEMENTS

The authors express their appreciation to Mitsubishi Gas Chemical Co., Mitsubishi Engineering-Plastics Corp. and

the US Army Research Office for their support of various aspects of this research.

REFERENCES

1. Yee, A. F. and Kambour, R. P., in *Proceedings of International Conference: Toughening of Plastics*. Plastics and Rubber Institute, London, 1978, p. 20.1.
2. Mallick, P. and Jennings, J., in *Proceedings of ANTEC 1988*. Society of Plastic Engineers, CT, 1988, p. 582.
3. Agrawal, C. M. and Pearsall, G. W., *Journal of Materials Science*, 1991, **26**, 1919.
4. Parker, D. S., Sue, H.-J., Huang, J. and Yee, A. F., *Polymer*, 1990, **31**, 2268.
5. Debier, D., Devaux, J., Legras, R. and Leblanc, D., *Polymer Engineering Science*, 1994, **34**, 613.
6. Chang, F.-C., Wu, J.-S. and Chu, L.-H., *Journal of Applied Polymer Science*, 1992, **44**, 491.
7. Wert, M. J., Saxena, A. and Ernst, H. A., *Journal of Testing and Evaluation (ASTM)*, 1990, **18**, 1.
8. Cheng, C., Hiltner, A., Baer, E., Soskey, P. R. and Mylonakis, S. G., *Journal of Applied Polymer Science*, 1994, **52**, 177.
9. Cheng, C., Peduto, N., Hiltner, A., Baer, E., Soskey, P. R. and Mylonakis, S. G., *Journal of Applied Polymer Science*, 1994, **53**, 513.
10. Cheng, C., Hiltner, A., Baer, E., Soskey, P. R. and Mylonakis, S. G., *Journal of Applied Polymer Science*, 1995, **55**, 1691.
11. Cheng, C., Hiltner, A., Baer, E., Soskey, P. R. and Mylonakis, S. G., *Journal of Materials Science*, 1995, **30**, 587.
12. Lee, C.-B. and Chang, F.-C., *Polymer Engineering Science*, 1992, **32**, 792.
13. Cheng, T.-W., Keskkula, H. and Paul, D. R., *Polymer*, 1992, **33**, 1606.
14. Kayano, Y., Keskkula, H. and Paul, D. R., *Polymer*, 1997, **38**, 1885.
15. Partidge, I., Sanz, C. and Bickerstaff, K., in *Proceedings of The Fifth Annual Meeting of the Polymer Processing Society*. Kyoto, Japan, 1989, p. 218.
16. Bernstein, H. L., *Fracture toughness of polycarbonate as characterized by the J-integral*. In *Elastic-Plastic Test Methods: The User's Experience (Second Volume), ASTM STP 1114*, ed. J. A. Joyce, ASTM, Philadelphia, 1991, p. 306.
17. Chung, W. N. and Williams, J. G., *Determination of J_{IC} for polymers using the single specimen method*. In *Elastic-Plastic Test Methods: The User's Experience (Second Volume), ASTM STP 1114*, ed. J. A. Joyce, ASTM, Philadelphia, 1991, p. 320.
18. Crouch, B. A. and Huang, D. D., *Journal of Materials Science*, 1994, **29**, 861.
19. Duffy, J. and Shih, C. F., in *Advances in Fracture Research. Proceedings of the 7th International Conference Fracture (ICF7)*, ed. K. Salama, K. Ravi-Chandar, D.M.R. Taplin and P. R. Rao, Pergamon, Oxford, 1989, p. 633.
20. Hashemi, S. and Williams, J. G., *Journal of Materials Science*, 1991, **26**, 621.
21. Huang, D. D., The application of the multispecimen J-integral technique to toughened polymers. In *Elastic-Plastic Test Methods: The User's Experience (Second Volume), ASTM STP 1114*, ed. J. A. Joyce, ASTM, Philadelphia, 1991, p. 290.
22. Mai, Y.-W. and Powell, P., *Journal of Polymer Science: Part B: Polymer Physics*, 1991, **29**, 785.
23. Takemori, M. T. and Narisawa, I., in *Advances in Fracture Research. Proceedings of the 7th International Conference Fracture (ICF7)*, ed. K. Salama, K. Ravi-Chandar, D. M. R. Taplin and P. R. Rao, Pergamon, Oxford, 1989, p. 2733.
24. Vu-Khanh, T., *Polymer*, 1988, **29**, 1979.
25. Wu, J. and Mai, Y.-W., *Journal of Materials Science*, 1993, **28**, 6167.
26. Vu-Khanh, T. and De Charentenay, F. X., *Polymer Engineering Science*, 1985, **25**, 841.
27. Paton, C. A. and Hashemi, S., *Journal of Materials Science*, 1992, **27**, 2279.
28. Zhou, Z., Landes, J. D. and Huang, D. D., *Polymer Engineering Science*, 1994, **34**, 128.
29. Huang, D. D. and Williams, J. G., *Journal of Materials Science*, 1987, **22**, 2503.
30. Huang, D. D., in *Proceedings of ANTEC 1991*, Society of Plastic Engineers, CT, 1991, p. 582.
31. Seidler, S. and Grellmann, W., *Journal of Materials Science*, 1993, **28**, 4078.
32. *E-399 Standard Test Method for Plane-Strain Fracture Toughness of Metallic Materials*. Annual Book of ASTM standards, American Society for Testing and Materials, Philadelphia, 1990.
33. *E-813 Standard Test Method for J_{IC}, A Measure of Fracture Toughness*. Annual Book of ASTM standards, American Society for Testing and Materials, Philadelphia, 1989.
34. Mai, Y.-W., *Polymer Communications*, 1989, **30**, 330.
35. Mai, Y.-W. and Cotterell, B., *International Journal of Fracture*, 1986, **32**, 105.
36. Mai, Y.-W., Cotterel, B., Horlck, R. and Vigna, G., *Polymer Engineering Science*, 1987, **27**, 804.
37. Hodgkinson, J. M. and Williams, J. G., *Journal of Materials Science*, 1981, **16**, 50.
38. Beauchamp, K. G. and Yuen, C. K., *Digital Methods for Signal Analysis*. George Allen & Unwin, Boston, 1979, p. 97.
39. Yee, A. F., *Journal of Materials Science*, 1977, **12**, 757.
40. Li, D., Yee, A. F., Chen, I.-W., Chang, S.-C. and Takahashi, K., *Journal of Materials Science*, 1994, **29**, 2205.
41. Sue, H.-J. and Yee, A. F., *Journal of Materials Science*, 1991, **28**, 0.
42. Broek, D., *Elementary Engineering Fracture Mechanics*. Noordoff International, Leyden, 1974, p. 96.
43. Bucknall, C. B., Heather, P. S. and Lazzeri, A., *Journal of Materials Science*, 1989, **16**, 2255.
44. Bucknall, C. B., Karpodinis, A. and Zhang, X. C., *Journal of Materials Science*, 1994, **29**, 3377.
45. Hertzberg, R. W., *Deformation and Fracture Mechanics of Engineering Materials*, 3rd edn. John Wiley & Sons, New York, 1989, p. 142.
46. Plati, E. and Williams, J. G., *Polymer Engineering Science*, 1975, **15**, 470.
47. Williams, J. G., *Fracture Mechanics of Polymers*. Ellis Horwood, Chichester, 1984.